

# Novel Blind Equalizer for Coherent DP-BPSK Transmission Systems: Theory and Experiment

Erwan Pincemin, Nicolas Brochier, Mehrez Selmi, Omid Zia Chahabi, Philippe Ciblat, and Yves Jaouën

**Abstract**—Adaptive blind equalization based on constant modulus algorithm is very efficient to carry out polarization separation and inter-symbol interference compensation in a coherent dual-polarization quaternary-phase-shift-keying transmission system. Its performance is, however, very poor when coherent dual-polarization binary-phase-shift-keying (BPSK) modulation is considered. In this letter, we propose a new blind equalizer adapted to any PSK constellation and we theoretically show its convergence. Experimental BER measurements and convergence analysis are performed in a 40 Gbps coherent dual-polarization BPSK system under different physical impairments. We show that our equalizer outperforms existing blind algorithms.

**Index Terms**—Coherent optical communications, binary-phase shift-keying, blind equalization, constant modulus algorithm.

## I. INTRODUCTION

COHERENT dual-polarization quaternary-phase-shift-keying (DP-QPSK) WDM long-haul transmission systems are now currently deployed at 40 and 100 Gbps [1], [2]. However, thanks to its higher robustness to fiber nonlinearities, 40 Gbps systems based on coherent dual-polarization binary-phase-shift-keying (DP-BPSK) represents a better long-haul transport solution when mixed 10/40 Gbps WDM systems are used [3]. Moreover, it is well-known that the constant modulus algorithm (CMA) performs efficiently polarization separation and inter-symbol interference compensation in DP-QPSK systems [4], [5]. In contrast, it fails for DP-BPSK. Indeed, the CMA equalizer requires a circularly-symmetric constellation (i.e.,  $E[s^2] = 0$  with  $s$  the transmitted symbol sequence). This assumption is not satisfied by BPSK [6]. Therefore, equalization algorithm adapted to DP-BPSK is required. A previous algorithm has been proposed in [7], but the carrier frequency offset (CFO) knowledge is necessary.

In this letter, we introduce a new blind equalizer, insensitive to CFO and adapted to any PSK constellation. We firstly prove theoretically that the proposed algorithm converges in any case. Secondly, its performance is evaluated through measurements on a 40 Gbps coherent DP-BPSK experiment corrupted

by various impairments, such as chromatic dispersion (CD) and polarization mode dispersion (PMD). The obtained results show a negligible system penalty.

## II. SYSTEM MODEL AND STATE-OF-THE-ART

Let  $y_{p,a}(t)$  (resp.  $y_{q,a}(t)$ ) be the continuous-time received signal on polarization  $p$  (resp.  $q$ ). By sampling this signal at twice the baud rate, we get the bivariate discrete-time signal:

$$\mathbf{y}_p(n) = \left[ y_{p,a}(nT_s), y_{p,a}\left(nT_s + \frac{T_s}{2}\right) \right]^T \quad (1)$$

where the subscript  $(\cdot)^T$  stands for the transposition, and  $T_s$  is the symbol duration. Let  $w_{x,y}(l)$  be the  $l$ -th component (of size  $1 \times 2$ ) of the fractionally-spaced equalizer (FSE) between polarizations  $x$  and  $y$ . Assuming the equalizer of length  $(L + 1)$ , its scalar output associated with polarization  $p$  writes as:

$$\begin{aligned} z_p(n) &= \sum_{l=0}^L \mathbf{w}_{p,p}(l) \mathbf{y}_p(n-l) + \mathbf{w}_{p,q}(l) \mathbf{y}_q(n-l) \\ &= \mathbf{w}_p^T \mathbf{y}^{(L)}(n) \end{aligned} \quad (2)$$

with  $\mathbf{w}_p = [\mathbf{w}_{p,p}(0), \dots, \mathbf{w}_{p,p}(L), \mathbf{w}_{p,q}(0), \dots, \mathbf{w}_{p,q}(L)]^T$  and

$$\mathbf{y}^{(L)}(n) = \left[ \mathbf{y}_p(n)^T, \mathbf{y}_p(n-1)^T, \dots, \mathbf{y}_p(n-L)^T, \mathbf{y}_q(n)^T, \mathbf{y}_q(n-1)^T, \dots, \mathbf{y}_q(n-L)^T \right]^T.$$

In [7], the authors have proposed a blind equalizer adapted to DP-BPSK relying on the minimization of the following cost function (for recovering polarization  $p$ ):

$$J_p(\mathbf{w}_p) = E \left[ |r_n^2 - e^{2j\Delta\theta}|^2 \right] \quad (3)$$

where BPSK symbol belongs to  $\{-1, 1\}$ ,  $\Delta\theta = 2\pi \Delta f T_s$  with  $\Delta f$  the CFO and  $r_n$  is defined by:

$$r_n = z_p(n) z_p^*(n-1). \quad (4)$$

Using the stochastic gradient-descent algorithm, the equalizer taps update is given as follows:

$$\mathbf{w}_p(n+1) = \mathbf{w}_p(n) - \mu \nabla J_p \quad (5)$$

with  $\mu$  the constant step-size, and:

$$\begin{aligned} \nabla J_p &= \left( r_n^2 - e^{2j\Delta\theta} \right) r_n^* z_p(n-1) \mathbf{y}^{*(L)}(n) \\ &\quad + \left( r_n^2 - e^{2j\Delta\theta} \right)^* r_n z_p(n) \mathbf{y}^{*(L)}(n-1). \end{aligned} \quad (6)$$

We note that this equalizer requires a prior knowledge of the CFO, and does not converge if its initial value is inaccurate.

Manuscript received February 7, 2013; revised July 15, 2013; accepted July 31, 2013. Date of publication August 15, 2013; date of current version August 30, 2013.

E. Pincemin, N. Brochier, M. Selmi, and O. Z. Chahabi are with the Department of Orange Labs Network, France Telecom, Orange Labs, Lannion 22300, France (e-mail: erwan.pincemin@orange.com; nicolas.brochier@orange.com; mehrez.selmi@orange.com; omid.ziachahabi@orange.com).

P. Ciblat and Y. Jaouën are with COMELEC, Telecom Paristech, Paris 75039, France (e-mail: philippe.ciblat@telecom-paristech.fr; yves.jaouen@telecom-paristech.fr).

Color versions of one or more of the figures in this letter are available online at <http://ieeexplore.ieee.org>.

Digital Object Identifier 10.1109/LPT.2013.2277604

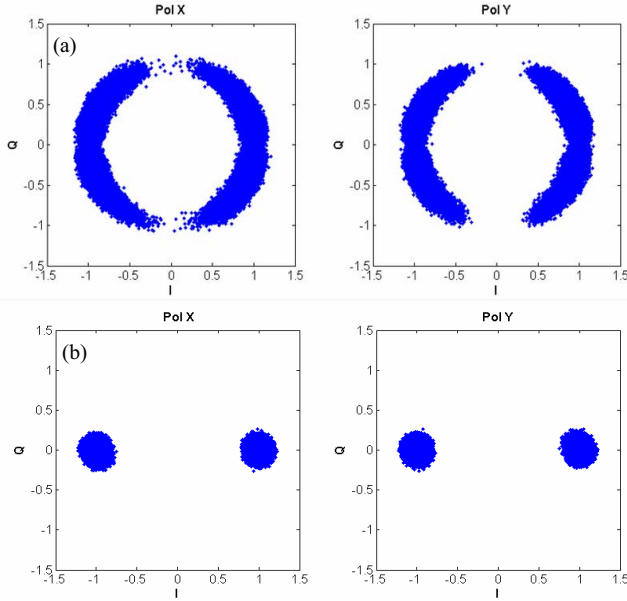


Fig. 1. Examples of measured DP-BPSK constellations (over  $10^6$  received symbols): (a) standard CMA equalizer, (b) proposed blind equalizer.

### III. PROPOSED EQUALIZER

Unlike [7], we propose a new blind equalizer which works without prior CFO estimation and for any PSK constellation, especially, BPSK. The proposed equalizer is obtained by the minimization of the following cost function:

$$J_p(\mathbf{w}_p) = E \left[ \left( |z_p(n)|^2 - 1 \right)^2 \right] - \left| E \left[ z_p(n)^2 \right] \right|^2. \quad (7)$$

The first term in the above expression represents the CMA and ensures that the equalizer output is located on a unit-radius circle. When BPSK is used, the second term forces the equalizer output to be noncircularly symmetric and thus close to BPSK ( $|E[z_p(n)^2]|^2 = 1$  for an ideal BPSK). So, this removes the undesirable configurations. Note that for higher-order PSK format, our additional term does not degrade the performance since it is close to zero and boils down standard CMA (cf. Fig. 1). The equalizer taps update is then given by Eq. (5), but with the following expression:

$$\nabla J_p = \left( 2 \left( |z_p(n)|^2 - 1 \right) z_p(n) - m_p(n) z_p^*(n) \right) \mathbf{y}^{*(L)}(n) \quad (8)$$

with  $m_p(n) = (1 - \delta) m_p(n-1) + \delta z_p^2(n)$ ,  $m_p(0) = 0$ , and  $\delta$  a forgetting factor whose value is between 0 and 1.

We hereafter prove that the proposed algorithm assuming infinite equalizer length removes completely the inter-symbol interference. As in [8], [10], and [11], by sake of simplicity, we limit our demonstration to the single-polarization configuration, received signal sampled at the baud rate, and noiseless case. Consequently,  $\mathbf{w}_p$  reduces to an infinite length scalar sequence  $w = \{w(l)\}_l$ . First of all, one can see that  $z(n) = \sum_l f(l) s(n-l)$  where  $s(n)$  corresponds to the transmit BPSK symbols and the filter  $f = \{f(l)\}_l$  represents the concatenation of the propagation and equalizer filters  $w$ . From now on, we mathematically consider that the cost function

$J$  depends on  $f$  rather on  $w$ . After tedious but straightforward algebraic manipulations, we obtain that:

$$J(f) = 1 + 2 \left( \sum_l u(l) \right)^2 + 2 \left( \sum_l v(l) \right)^2 - 2 \sum_l u(l)^2 - 2 \sum_l v(l)^2 + 4 \sum_l u(l) \sum_l v(l) - 4 \sum_l u(l) v(l) - 2 \sum_l (u(l) + v(l)) \quad (9)$$

with  $u(l) = \text{Re}\{f(l)\}^2$  and  $v(l) = \text{Im}\{f(l)\}^2$ . By forcing the filter  $f$  to be unit-energy, the criterion simplifies as follows:

$$J(f) = \sum_{k \neq l} (u(k)u(l) + v(k)v(l) + 2u(k)v(l)) \quad (10)$$

where constant terms have been removed. As  $u(l)$  and  $v(l)$  are positive, the minimum of the cost function  $J$  is achieved if and only if:

$$\sum_{k \neq l} u(k)u(l) = \sum_{k \neq l} v(k)v(l) = \sum_{k \neq l} u(k)v(l) = 0 \quad (11)$$

which implies that the terms  $u(k)u(l)$ ,  $v(k)v(l)$  and  $u(k)v(l)$  vanish as soon as  $k$  is different from  $l$ . These constraints can be satisfied if and only if i) the non-null terms of  $u$  and  $v$  are obtained at the same indices, ii) these non-null terms are obtained only for one index. We have thus proven that  $f$  is a filter with only one tap and the inter-symbol interference has been entirely removed. Extension to dual-polarization case with received signal sampled at twice the baud rate can be done easily.

### IV. RESULTS AND DISCUSSION

The performance of the proposed equalizer is studied owing to the 42.8 Gbps DP-BPSK experiment set-up, described in Fig. 2. The DP-BPSK transmitter is fed by a 100 kHz external cavity laser (ECL) at 1550.12 nm.  $2^{15}-1$  pseudo-random bit sequences (PRBS) with a peak-to-peak amplitude voltage equal to  $2V_\pi$  are used to drive the Mach-Zehnder modulator (MZM). The MZM is polarized to the null transmission point. The polarization-multiplexing unit is constituted of a 10-ns temporal delay which has for role to de-correlate the two replica of the BPSK signal which are polarization-multiplexed. The CD emulator is constituted of three Teraxion fibre Bragg grating-based modules of 10000 ps/nm each. The PMD emulator (General Photonics PMD-1000) is able to generate both differential group delay (DGD) up to 182 ps, and 2<sup>nd</sup>-order PMD (SOPMD) up to 8159 ps<sup>2</sup>. A polarization scrambler (PS) makes vary randomly the state of polarization of the signal at 70°/ms speed.

At the receiver side, a phase and polarization diversity coherent detector is used to separate the two in-phase and quadrature tributaries as well as the two polarization components. The four obtained electrical baseband signals are then captured by a 50 GSa/s digital oscilloscope (DPO). The acquired waveforms (2 millions of samples per run) are processed off-line. Digital signal processing (DSP) consists in signal re-sampling at twice the symbol rate, FIR filter-based temporal domain equalizer for CD compensation [5], adaptive blind equalizer for polarization demultiplexing and

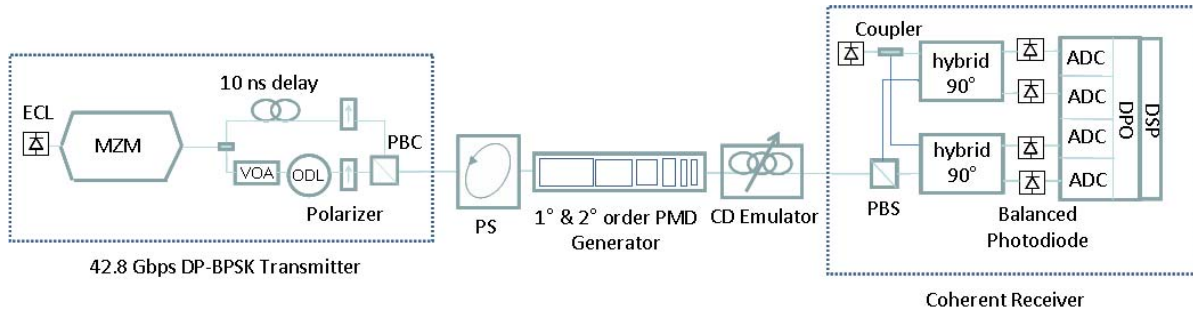


Fig. 2. Experimental set-up with the 42.8 Gbps DP-BPSK transmitter, polarization scrambler, PMD and CD emulators, and the coherent receiver (ECL: external cavity laser, MZM: Mach-Zehnder modulator, VOA: variable optical attenuator, ODL: optical delay line, PBC: polarization beam combiner, PS: polarization scrambler, PMD: polarization mode dispersion, CD: chromatic dispersion, PBS: polarization beam splitter, ADC: analogue-to-digital converter, DPO: digital phosphor oscilloscope, DSP: digital signal processing).

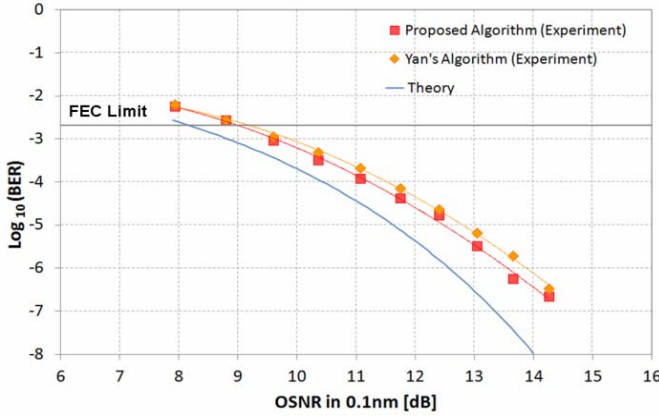


Fig. 3. BER vs. OSNR in the back-to-back configuration for the proposed equalizer, and for the Yan's equalizer. The BER vs. OSNR curve foreseen by theory is used here as a reference.

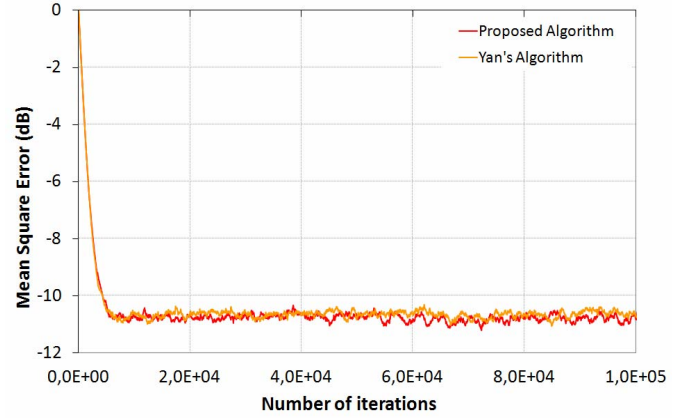


Fig. 4. Estimated mean square error (in dB) vs. iteration number for the proposed equalizer, and for the Yan's equalizer.

PMD compensation [5]–[8], CFO compensation [9], Viterbi-Vibert carrier phase estimation [4], differential decoding and finally symbol decision. The BER value results from an averaging over 50 acquisitions.

#### A. Back-to-Back Performance

In the back-to-back (BtB) configuration, only the polarization scrambler is inserted. The signal is blended with an amplified spontaneous emission (ASE) noise source. The convergence phase is ensured by using 20% of the received sequence. The equalizer parameters have been optimized as follows:  $\delta = 0.7$  and  $\mu = 10^{-3}$ . The FIR filters of the adaptive blind equalizer have 15 taps, while the carrier phase estimator uses data blocks of 17 samples. Fig. 3 shows the BER as a function of the optical signal to noise ratio (OSNR). The BER vs. OSNR curve foreseen by theory is taken here as a reference. BER vs. OSNR curves are plotted for the two described algorithms. Fig. 3 shows that the proposed algorithm is very efficient, and is slightly better than the Yan's algorithm [7]. The FEC limit (at  $\text{BER} = 2 \times 10^{-3}$ ) is obtained for a 9-dB OSNR: this value is close to the theoretical limit fixed at 8.2 dB.

In order to evaluate the convergence of the proposed algorithm, the mean square error is plotted as a function of the number of iterations over the polarization  $x$  in Fig. 4.

The estimated mean square error ( $\widehat{MSE}$ ) is defined as follows:

$$\widehat{MSE}_p(n+1) = \beta \widehat{MSE}_p(n) + (1-\beta) |z_p(n) - \hat{d}_p(n)|^2 \quad (12)$$

$\beta$  is a forgetting factor equal to 0.999, and  $\hat{d}_p$  is the decided symbol after the CFO compensation and Viterbi-Vibert carrier phase estimation. For the two algorithms under study, less than 5000 iterations are necessary to reach the steady state, which corresponds to a  $\widehat{MSE}$  value of  $\sim -11$  dB. It is interesting to note that this steady state is very stable during the time, and that the proposed equalizer and the Yan's algorithm have a very similar behavior.

#### B. Performance in the Presence of Carrier Frequency Offset

The proposed equalizer, by construction, does not require any prior knowledge of the CFO value, at the opposite of the Yan's algorithm. However, its performance can be affected by the CFO value. In order to compare the equalizer efficiencies, CFO has been precisely emulated by detuning the wavelengths of the transmitter laser and local oscillator.

The BER as a function of the CFO values have been plotted in Fig. 5 for the two equalizers under study for an OSNR  $\sim 11.2$  dB. The BER is kept below the FEC limit for CFO in the range of  $\pm 1.5$  GHz for the proposed algorithm, while Yan's algorithm tolerates only a CFO range of  $\pm 0.4$  GHz.

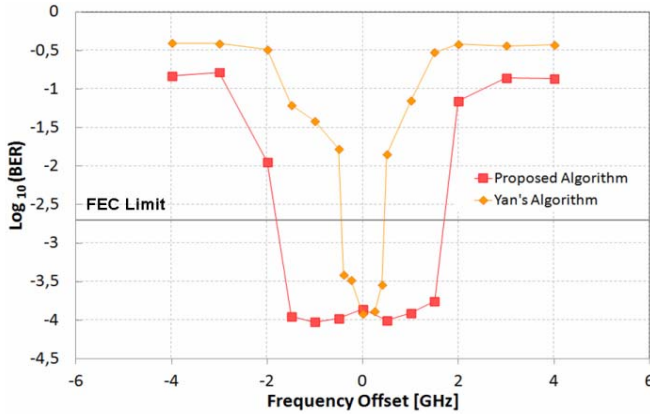


Fig. 5. BER vs. carrier frequency offset after equalization using both the proposed algorithm and the Yan's algorithm.

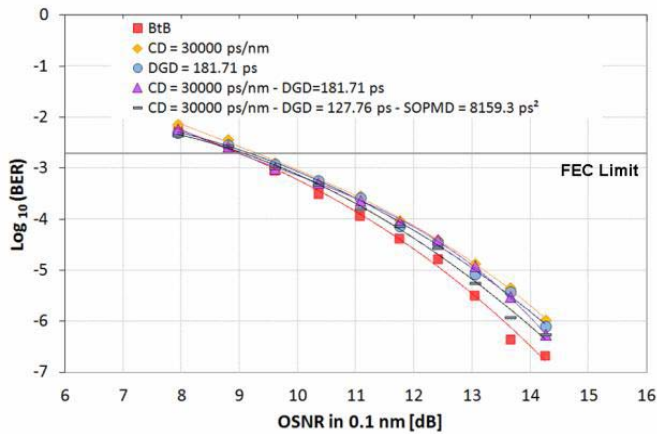


Fig. 6. BER vs. OSNR in various configurations of CD, DGD, and SOPMD combination (polarization scrambling speed  $\sim 70^\circ/\text{ms}$ ).

### C. Robustness Against CD, DGD, SOPMD Under Fast PS

The main task of the adaptive equalization is to compensate for polarization-dependent effects, such as DGD and SOPMD. The BER vs. OSNR curves are measured with our proposed equalizer in various configurations (see Fig. 6). We first introduce 30000 ps/nm of CD and/or  $\sim 182$  ps of DGD. The most detrimental configuration with 30000 ps/nm of CD,  $\sim 128$  ps of DGD and  $\sim 8159$  ps<sup>2</sup> of SOPMD is also evaluated. Note that our PMD emulator does not permit to choose independently any value of DGD and SOPMD: we have thus deliberately chosen the worst value of SOPMD ( $\sim 8159$  ps<sup>2</sup>) that the emulator can generate. As depicted in Fig. 6 below, the OSNR penalties after compensation of CD, DGD, and SOPMD with respect to the BtB case are negligible at the FEC limit ( $< 0.5$  dB) and are less than 1 dB for the other BER values, demonstrating clearly the efficiency of our equalizer.

To still confirm the convergence, the  $\overline{MSE}$  is plotted as a function of the number of iterations over the polarization  $x$  in Fig. 7. In presence of CD, DGD, or a mix of them, the convergence time is similar to that observed in the BtB case: less than 5000 iterations are required to reach the steady state. Even in the most severe configuration where 30000 ps/nm of CD,  $\sim 128$  ps of DGD and  $\sim 8159$  ps<sup>2</sup> of SOPMD are emulated, the  $\overline{MSE}$  plot has the same profile

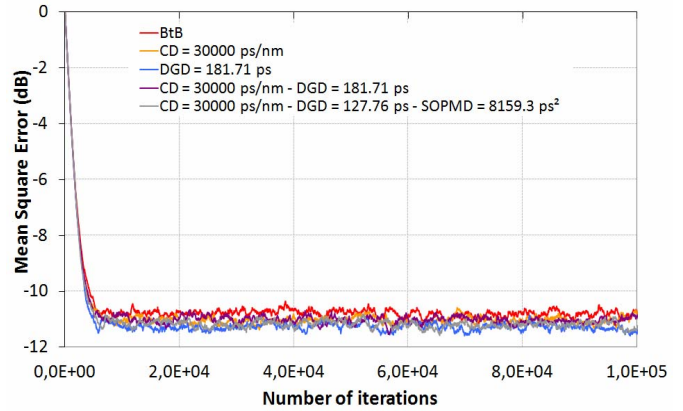


Fig. 7. Estimated mean square error (in dB) vs. iteration number for the proposed equalizer in various configurations of CD, DGD, and SOPMD combination (polarization scrambling speed  $\sim 70^\circ/\text{ms}$ ).

than those corresponding to the other cases, confirming the robustness of the proposed equalizer.

## V. CONCLUSION

We have proposed a new adaptive blind equalizer dedicated specifically to DP-BPSK transmission systems which does not require any prior knowledge of CFO. In addition, the proof of equalizer convergence has been developed. Compared to Yan's algorithm, we are much more robust to ASE noise and CFO. Experimental results show that our algorithm successfully equalizes the 40 Gbps DP-BPSK system disturbed by CD, DGD and SOPMD under fast polarization scrambling. The experimental convergence analysis also confirms the robustness of our equalizer to the most severe propagation conditions.

## REFERENCES

- [1] (2011). *Alcatel-Lucent 1830 PSS Brochure* [Online]. Available: <http://www.alcatel-lucent.com>
- [2] (2013). *Ciena 6500 Product Data Sheet* [Online]. Available: <http://www.ciena.com>
- [3] M. Salsi, et al., "Experimental comparison between binary and quadrature phase shift keying at 40 Gbps in a transmission system using coherent detection," in *Proc. ECOC*, 2010, paper Mo.2.C.5.
- [4] D. S. Ly-Gagnon, S. Tsukamoto, K. Katoh, and K. Kikuchi, "Coherent detection of optical quadrature PSK signals with carrier phase estimation," *J. Lightw. Technol.*, vol. 24, no. 1, pp. 12–21, Jan. 2006.
- [5] S. J. Savory, "Digital filters for coherent optical receivers," *Opt. Express*, vol. 16, no. 2, pp. 804–817, 2008.
- [6] C. B. Papadias, "On the existence of the undesirable global minima of Godard equalizers," in *Proc. ICASSP*, 1997, pp. 3941–3942.
- [7] M. Yan, Z. Tao, H. Zhang, W. Yan, T. Hoshida, and J. C. Rasmussen, "Adaptive blind equalization for coherent optical BPSK system," in *Proc. ECOC*, 2010, paper Th.9A.4.
- [8] D. Godard, "Self recovering equalization and carrier tracking in two dimensional data communications systems," *IEEE Trans. Commun.*, vol. 28, no. 11, pp. 1867–1875, Nov. 1980.
- [9] A. Leven, N. Kaneda, and U. V. Koc, "Frequency estimation in intradyne reception," *IEEE Photon. Technol. Lett.*, vol. 19, no. 6, pp. 366–368, Mar. 15, 2007.
- [10] O. Shalvi and E. Weinstein, "New Criteria for blind deconvolution of non-minimum phase systems," *IEEE Trans. Inf. Theory*, vol. 36, no. 2, pp. 312–321, Mar. 1990.
- [11] S. Houcke and A. Chevreuil, "Characterization of the undesirable global minima of the Godard cost function: Case of noncircular symmetric signals," *IEEE Trans. Commun.*, vol. 54, no. 5, pp. 1917–1922, Jun. 2007.